


**Controlled switching of a single CuPc molecule on Cu(111) at low temperature**Sweetlana Fremy-Koch,<sup>1,\*</sup> Ali Sadeghi,<sup>2</sup> Rémy Pawlak,<sup>1</sup> Shigeki Kawai,<sup>1,†</sup> Alexis Baratoff,<sup>1</sup> Stefan Goedecker,<sup>1</sup> Ernst Meyer,<sup>1</sup> and Thilo Glatzel<sup>1,‡</sup><sup>1</sup>*Department of Physics, University of Basel, Klingelbergstrasse 82, 4056 Basel, Switzerland*<sup>2</sup>*Department of Physics, Shahid Beheshti University, G.C., Evin, 19839-63113 Tehran, Iran* (Received 6 November 2015; revised manuscript received 2 October 2019; published 24 October 2019)

Low temperature measurements of the tunneling current as a function of the applied bias voltage have been performed on a dense constant-height grid above individual copper phthalocyanine molecules adsorbed on a Cu(111) surface. By appropriate tuning of the applied bias, the molecule can be reversibly switched between two configurations in which pairs of opposite maxima appear rotated by  $90^\circ$  in the tunneling current map. The underlying conformations are revealed by density functional calculations including van der Waals interactions: a  $C_{2v}$  symmetric ground state and two energetically equivalent states, in which the molecule is twisted and rotated around its center by  $\pm 7^\circ$ . For tip biases above 200 mV position-dependent current switching is observed, as in previous measurements of telegraph noise [Schaffert *et al.*, *Nat. Mater.* **12**, 223 (2013)]. In a small voltage interval around zero the measured current becomes bistable. Switching to a particular state can be initiated by sweeping the voltage past well-defined positive and negative thresholds at certain positions above the molecule or by scanning at constant current and a reduced reverse bias.

DOI: [10.1103/PhysRevB.100.155427](https://doi.org/10.1103/PhysRevB.100.155427)**I. INTRODUCTION**

Organic molecules with switching properties are currently investigated intensely within the field of molecular electronics [1–3], particularly for their prospects for memory elements [4,5]. Molecular switches are characterized by a bistable configuration, such as the charge state [6–11] or the conformation of a molecule [12–15]. The bistability can be reversibly controlled externally, for instance, by supplying an interaction force [16,17], light [18–20], electrons [21–23], or even by inducing a single proton transfer [24,25]. Nowadays, scanning tunneling (STM) and atomic force microscopy (AFM) techniques [26–28] serve as unique tools to address and control molecular properties at the nanoscale. While in AFM forces can be controlled accurately to manipulate molecules and atoms [29–33], in STM any required force can only be indirectly controlled by the tip-sample distance and voltage [34]. In addition, inelastic tunneling electrons have been used to induce a large variety of manipulations. Such inelastic processes can excite molecular vibrations [35] and may induce desorption [36], bond formation and dissociation [37,38], molecular rotation [39–42], and also lateral movement of adsorbed molecules [43–45]. For instance, inelastic tunneling electrons excite a molecular vibration that couples to one of the hindered rotational modes, resulting in a rotational movement of the molecule. By injecting electrons at certain

low-symmetry positions of the molecule, movement can, in principle, be controlled [46].

Here we demonstrate that tunneling electrons can be tuned to induce selectively two rotational states of individual copper phthalocyanine (CuPc) molecules on a Cu(111) surface. Bias-dependent spectroscopic data  $I_t(x, y, U_{\text{tip}})$ , acquired above isolated CuPc molecules on the Cu(111) surface, will be discussed. Previous low temperature STM measurements on the same system by Karacuban *et al.* [47] pointed out that at a negative sample bias voltage individual molecules appear with two opposite lobes blurred by current noise. By analyzing the telegraph character of the noise as a function of recording time, they demonstrated that isolated CuPc molecules repeatedly switched between two states when the tip was placed above a blurred lobe. Subsequently, the same group identified the high-current state with the lowest energy configuration of the molecule, in which the opposite lobes in question are aligned perpendicular to a  $\langle 1\bar{1}0 \rangle$  direction of the Cu(111) substrate, and the low-current state with two metastable configurations in which the same lobes are rotated by  $\pm 7^\circ$  [48,49]. However, we show that this assignment has to be partly revised in the light of additional details revealed by our experiments.

The same authors found good agreement with a specific inelastic tunneling mechanism which indirectly couples frustrated rotations confined around the three above-mentioned low-energy configurations. Then noise arises from the multitude of preferentially excited high-energy rotational states and their subsequent stochastic relaxation to the three low-energy configurations. As for most manipulation processes induced by inelastic tunneling, this mechanism is especially efficient whenever the Fermi level of the tip is swept past one of the molecule-derived electronic resonances broadened and down-shifted by coupling to the substrate. This is in particular

\*Present address: Endress+Hauser AG+Co. KG, Colmarer Straße 6, 79576 Weil am Rhein, Germany.

†Present address: International Center for Materials Nanoarchitectonics, National Institute for Materials Science, 1-1 Namiki Tsukuba, Ibaraki 305-0044, Japan.

‡thilo.glatzel@unibas.ch

true for the slightly split and doubly occupied LUMO-derived resonances which are closest to the Fermi level of Cu(111) upon adsorption.

We extended the tip-sample bias voltage interval to both polarities and imaged the molecule either in its ground state or in the rotated configuration and thus could unambiguously correlate the current with a particular state. The associated conformations determined by first principles calculations reveal important differences between the relaxed adsorption geometries of the ground and the rotated states, which are also reflected in the STM images. We also show that within the same bias interval a molecule in one configuration can be controllably switched to the other one. The bistability exhibits the same position sensitivity as the above-mentioned noise, but occurs in a range where the stochastic rotational inelastic excitation mechanism is deemed inefficient.

## II. EXPERIMENTAL AND CALCULATION DETAILS

Experiments were performed with a commercial LT-STM/AFM from Omicron Nanotechnology at 5 K, a base pressure of  $<10^{-10}$  mbar, and equipped with a *qPlus* sensor used here only for STM measurements. The bias voltage was applied to the tungsten tip, which was decorated with Cu atoms by indenting it into the clean copper substrate. The Cu(111) surface was prepared by several cycles of  $\text{Ar}^+$  sputtering and subsequent annealing at  $\approx 770$  K. CuPc molecules were thermally deposited from a Knudsen cell at 583 K onto the substrate kept at room temperature.

Density functional theory (DFT) within the generalized gradient approximation in the PBE form [50] and corrected for van der Waals interactions [51] was employed in the calculations. The substrate (111) surface was modeled with a four-layer slab of area  $17.9 \times 18.0 \text{ \AA}^2$ , each layer containing 56 copper atoms, and a vacuum of thickness  $20 \text{ \AA}$  to separate the spurious periodic images of the slab in the normal-to-surface direction. A plane-wave basis set with a cutoff of 300 eV, a  $2 \times 2 \times 1$   $k$  mesh, and the projector-augmented wave (PAW) method [52,53] as implemented in the VASP code [54–57] were used. Keeping the bottom layer of the slab frozen, other atoms of the slab or molecule were relaxed until any residual force falls below  $0.02 \text{ eV/\AA}$ .

## III. RESULTS

At low submonolayer coverages, CuPc individually adsorbs on the Cu(111) surface, as shown in the overview constant-current STM image in Fig. 1(c). They adopt a flat-lying configuration, but two out of the four lobes of each molecule are along either of the three symmetry equivalent directions  $[\bar{1}\bar{1}0]$ ,  $[0\bar{1}\bar{1}]$ , and  $[\bar{1}0\bar{1}]$  of Cu(111), as marked by circles. In the gas phase, CuPc possesses  $D_{4h}$  symmetry, as can be seen from the chemical structure in Fig. 1(a). However, upon adsorption on Cu(111) the symmetry of CuPc is reduced to  $C_{2v}$ , as expected in view of the different symmetries between the surface and the molecule [47] and confirmed by our DFT calculations which indicate strong molecule-substrate interactions of an adsorption energy of  $\approx 5.59 \text{ eV/molecule}$ . In agreement with Schaffert *et al.* [48], our calculations (albeit with a different functional) predict that in the energetically

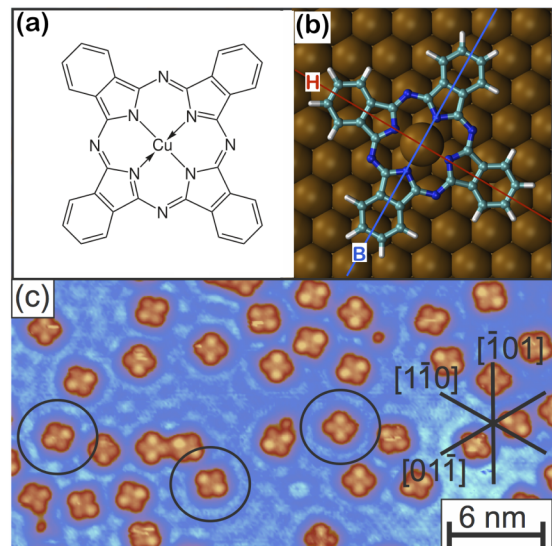


FIG. 1. (a) Chemical structure of copper phthalocyanine (CuPc). (b) Lowest energy adsorption configuration according to DFT calculations: the central Cu atom and two benzene rings are located above substrate bridge sites and define the B axis of the molecule, while the other two benzene rings are stabilized above hollow sites to define the molecular H axis. (c) STM topographic image of CuPc on Cu(111) at 5 K. Measurement parameters:  $U_{\text{tip}} = -200 \text{ mV}$ ;  $I_t = -30 \text{ pA}$ . The gas-phase  $D_{4h}$  symmetry of the molecules is reduced to  $C_{2v}$ . The flat-lying molecules adopt three different orientations along the  $[\bar{1}\bar{1}0]$ ,  $[0\bar{1}\bar{1}]$ , and  $[\bar{1}0\bar{1}]$  substrate directions marked by circles and act as charged scatterers for electrons injected into unoccupied surface states.

most favorable adsorption configuration the central Cu of the molecule sits at a substrate bridge position [see Fig. 1(b)]. One pair of the opposing terminal benzol rings are also centered on the surface bridge positions and hence are called B lobes hereafter. The other pair of benzol rings are centered atop the substrate hollow sites and called H lobes. Based on our DFT calculations, the B lobes stay further away from the surface as compared to the H lobes and are therefore assigned to the lobes appearing with brighter contrast in the STM image in Fig. 1(c). For convenience, we call the molecular axis that passes through the centers of the two B lobes as the B axis and indicate it by a blue line. The B axis is along the closely packed row of the copper atoms, i.e.,  $(\bar{1}\bar{1}0)$ , and represents the brighter lobes in the STM image of panel (c). The perpendicular direction is indicated by a red line and shows the other molecular axis, called H axis, which passes through the H lobes, i.e., the less bright lobes.

Figure 2 presents tunneling current data extracted from a three dimensional spectroscopy data set. To acquire such a set a two dimensional grid was predefined above the surface, and at each grid point  $(x, y)$ , an  $I_t(U_{\text{tip}})$  curve was recorded at constant height (20 pm above the STM setpoint of  $I_t = -30 \text{ pA}$  at  $U_{\text{tip}} = -150 \text{ mV}$ ), resulting in  $43 \times 43 \times 128$  measurement points. Between each bias sweep (6.4 s in each direction), feature-tracked tip positioning was activated for 10 s above a bright B lobe in the STM image to compensate residual long-term drift and creep [58–60]. The current sampling time per pixel at each position and voltage was 50 ms.

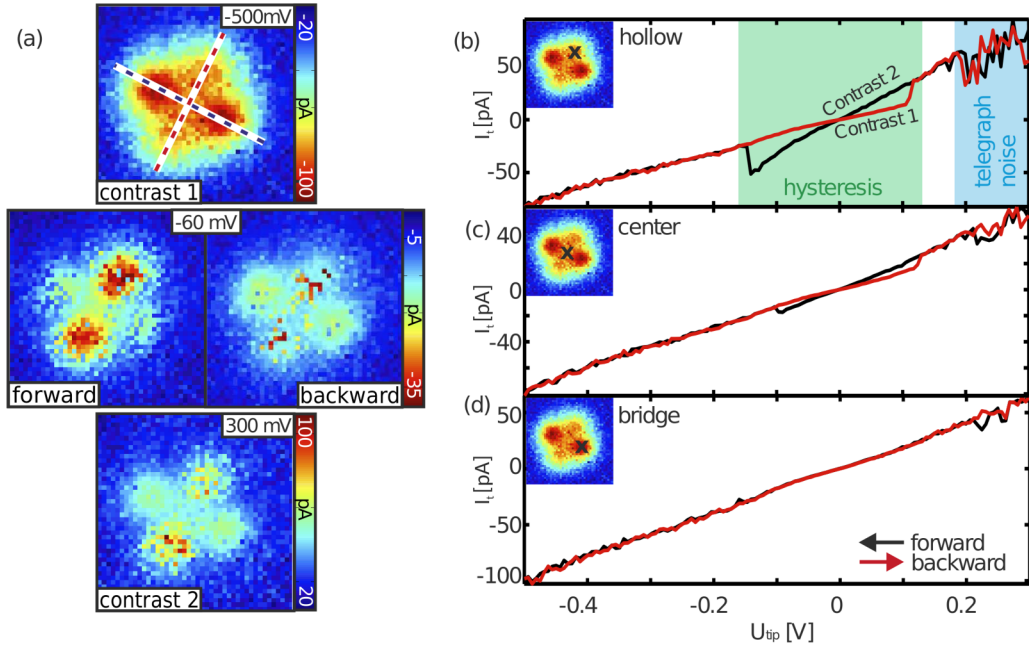


FIG. 2. (a) Constant height maps of the tunneling current of CuPc on Cu(111) at different tip voltages revealing a bias-dependent contrast transition, size  $2.5 \times 2.5$  nm<sup>2</sup>. (b)–(d) Single  $I_t(U_{tip})$  curves extracted above the molecular center, above a B and above a H lobe (see black crosses in the inset maps recorded at  $-500$  mV). Two position selective characteristic phenomena related to the contrast transition are apparent: telegraph noise (blue area) and a hitherto unobserved current hysteresis around zero bias (green area).

Figure 2(a) shows characteristic tunneling current maps above an individual molecule extracted from the  $I_t(x, y, U_{tip})$  data set at three different voltages. Note that the color scale, individually adjusted for each map, reflects variations of the absolute current. The observed pattern changes depending on the bias sweep direction, as seen in the representative images extracted at  $U_{tip} = -60$  mV. The map extracted at  $U_{tip} = -500$  mV, whose appearance coincides with the molecules imaged in Fig. 1(c), defines *Contrast 1* (bright B lobes). In the  $U_{tip} = 300$  mV map, which defines *Contrast 2*, the absolute current is slightly higher on the other pair of opposing H lobes. Within a bistable range around zero bias the current typically changes smoothly, as seen in the  $I_t(U_{tip})$  characteristics shown in Figs. 2(b)–2(d). Switching from one contrast to the other happens at about the same positive and negative bias voltages as in those characteristics. Focusing on the background colors of the lobes in the  $-60$  mV maps (rather than on the occasional noise spikes), one recognizes that the absolute current is higher above the (red) H lobes (*Contrast 2*) in the forward sweep direction defined in Fig. 2(d), while it is higher above the (green) B lobes in the backward direction (*Contrast 1*). The same difference appears in other maps extracted at other voltages in the bistable range.

Further details of the transition are revealed in Figs. 2(b)–2(d), showing pairs of representative forward and backward  $I_t(U_{tip})$  curves extracted at three characteristic positions above the molecule: the molecule center, a benzol ring above a substrate bridge site (B lobe), and one above a substrate hollow site (H lobe). Here, forward means that the tip bias was ramped from  $+300$  to  $-500$  mV and backward vice versa. The curves extracted above the H lobe in Fig. 2(b) exhibit two characteristic features: telegraphlike noise at positive tip bias polarity of  $U_{tip} > 200$  mV and a hysteretic range

between  $U_{tip} \approx -150$  and  $110$  mV with two distinct jumps of the current around those thresholds. For the curve extracted above the molecule center [Fig. 2(c)], both phenomena are still observed, albeit with notably smaller magnitude. The hysteresis interval shrinks from  $\approx 260$  to  $\approx 200$  mV, and the current jumps are reduced to  $\approx 5$  pA. Finally, above a B lobe [Fig. 2(d)], only weak telegraph noise and no current hysteresis are observed. Apart from hysteresis and telegraph noise all curves exhibit ohmic behavior, typical for molecules that are strongly bound to metal substrates.

#### IV. DISCUSSION

The current telegraph noise is identified by jumps between constant levels as a function of time at a fixed voltage as it was shown by Schaffert *et al.* [48]; here the noise appears as the voltage is slowly and incrementally swept. Such random signals are assigned to a random jump between two distinct conformations of the molecule. The position sensitive telegraph noise of CuPc on Cu(111) was explained by an athermal activation of frustrated rotations of the molecules by  $\pm 7^\circ$  around their center driven by inelastic tunneling [48,49]. Since the  $\pm 7^\circ$  rotations lead to two equivalent conformations, we assign the telegraph noise to random jumps between the two  $\pm 7^\circ$  rotated conformations passing in every jump the  $0^\circ$  position, corresponding to the excited and ground states of the molecule, respectively. The fact that mainly the benzol rings centered on the hollow sites (H lobes) display telegraph noise originates from the stronger local adsorption interactions of those rings. According to the calculations illustrated in Figs. 3(c) and 3(d) these rings are relaxed more strongly towards the substrate. This also is consistent with the predicted

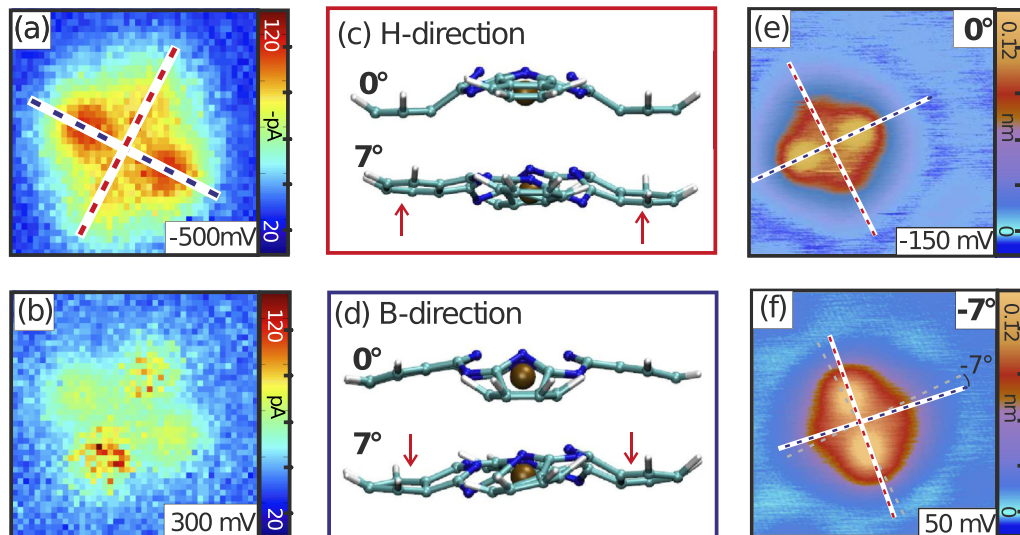


FIG. 3. Interpretation of the contrast change as a frustrated rotation of the CuPc molecule around its center. (a), (b) Constant height maps from Figs. 2(a) and 2(b) at  $-500$  mV, and  $300$  mV, but with identical color coding. (c), (d) Side views of the DFT calculated adsorption geometries in the symmetric configuration and that rotated by  $7^\circ$ ; out of plane displacements are magnified by a factor of four for better visualization. The direction of local height changes of the H lobes (c) and B lobes (d) are indicated by arrows. (e), (f) Constant current STM images demonstrating frustrated rotation induced by switching the bias between repeated scans over a molecule. Parameters: (e)  $U_{\text{tip}} = -150$  mV,  $I_t = -20$  pA; (f)  $U_{\text{tip}} = 50$  mV,  $I_t = 20$  pA.

larger local density of states of the split LUMO level aligned with the H axis [49].

Position sensitive hysteresis in  $I_t(U_{\text{tip}})$  curves have also previously been observed for single molecules nearly decoupled by ultrathin insulating films from metal substrates or adsorbed on a semiconducting surface and attributed to charging effects [6,61,62]. In the present case of a single CuPc molecule chemisorbed on a metal, however, the observed hysteresis cannot be due to molecular ion formation because such states, which would correspond to molecular resonances, are strongly broadened in energy, and hence are extremely short lived. For applied bias voltages within the bistable interval ( $\approx -150$  to  $110$  mV), the molecule resides either in the  $\pm 7^\circ$  rotated or in the unrotated state, as opposed to positive tip voltages beyond  $200$  mV, where telegraph noise related features are observed. Starting the voltage sweep from the right in the positive tip bias range above the H lobe [black curve in the upper panel of Fig. 2(b)], the molecule repeatedly switches between the metastable rotated conformations (high current) passing in every event the ground state (low current). This blue-shaded range is labeled telegraph noise. Then, within the bistable bias interval (green-shaded range labeled hysteresis), *Contrast 2* is maintained before it switches back to *Contrast 1* at  $\approx -150$  mV. At negative tip voltages the stable ground state is maintained. Along the backward sweep (red curve from left to right) *Contrast 1* is maintained throughout the bistable range, until it switches back to *Contrast 2* at  $\approx 110$  mV, followed by telegraph noise (sampled at each bias pixel over  $50$  ms) for  $U_{\text{tip}} > 200$  mV.

In order to check which configuration corresponds to *Contrasts 1* and *2*, the images of Fig. 2(a) are replotted in Figs. 3(a) and 3(b) in the  $[20, 120]$  pA range with identical color coding for both polarities. Note that the image showing *Contrast 1* (negative tip bias) has been plotted in units  $-\text{pA}$  rather

than pA. In this manner, the difference between the magnitudes of the tunneling current becomes obvious regardless of the current direction and can be more easily correlated with changes in relative heights from our DFT calculations. Compared to *Contrast 1* in Fig. 3(a), the two H lobes become brighter for *Contrast 2*, while the B lobes become darker. Because these two constant height maps were extracted from the same spectroscopy data, the contrast changes for the H and B lobes can be predominantly attributed to height changes of local parts of the molecule. The fact that the H lobes become brighter suggests that, compared to *Contrast 1*, these lobes lie further from the surface, while the B lobes are closer to the surface. It seems that a local chemical decoupling from the H sites of the substrate surface leads to an enhanced expansion of the LUMO, i.e., a brighter spot in STM, over the H lobes.

This observation is consistent with the conformational change upon rotation by  $\pm 7^\circ$  predicted by our DFT calculations. Side views (projected on a plane containing the H or B axis) of the calculated adsorption geometries for the symmetric and the rotated configurations are shown in Figs. 3(c) and 3(d). As also suggested by the changes between the STM images, the two benzol rings on the B axis [Fig. 3(d)] become closer to the substrate and slightly tilted in opposite directions after the  $7^\circ$  rotation. The rings on the H axis are also tilted, lifted up, and finally lie further from the surface [Fig. 3(c)]. This rotated adsorption geometry has so far only been observed for molecular films with coverages close to one monolayer [63], where molecule surface and the intermolecular interactions strongly compete. The full voltage dependent rotational behavior of the CuPc is shown schematically in Fig. 4. Comparing the results to those of Schaffert *et al.* [48] it is obvious that by varying the voltage only in the positive tip bias range (negative sample bias) the molecular appearance will remain in the high-current state following the

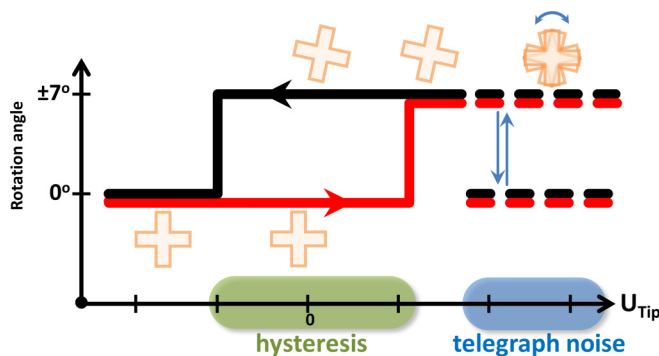


FIG. 4. Schematic representation of the voltage dependent rotation of the CuPc molecule. Applying a positive tip bias voltage above a certain threshold the molecule randomly jumps between the two  $\pm 7^\circ$  rotated conformations passing in every jump the  $0^\circ$  position in the telegraph noise region. By reducing the voltage either the  $+7^\circ$  or  $-7^\circ$  rotated conformation is adopted (for a better overview only one of the two orientations is shown) before the molecule switches to the  $0^\circ$  position at a certain negative tip voltage. Contrarily, while increasing the voltage from negative to positive tip biases the molecule stays in the  $0^\circ$  position until it switches again to one of the rotated states at positive tip bias values.

black forward curve from the right to the left. Therefore, the assignment of the high-current state to the ground state of the molecule has to be redefined since the tip bias has first to become negative to switch the molecule back to the unrotated ground state which is stable in appearance. Nevertheless, this new assignment does not affect the thorough noise analysis made by the same authors [48].

Our observation of a bistable bias range especially above the H lobes allows us to controllably switch individual molecules between the ground state and rotated state by sweeping the bias in opposite directions. Alternatively, a molecule can be switched by repeated scanning at opposite bias voltages, as illustrated in Figs. 3(e) and 3(f). In Fig. 3(e) the molecule appears in its symmetric conformation. By scan-

ning the same molecule with a positive bias of 50 mV instead, the molecule is switched into the metastable configuration, here rotated by  $-7^\circ$ , as indicated by the gray dashed lines. In this configuration, the benzol rings sitting on the surface hollow sites appear brighter, so that the change of the contrast pattern corresponds to an apparent rotation by about  $90^\circ$  (actually  $83^\circ$ ).

## V. CONCLUSION

In summary, we have observed a controllable bias-dependent switching of isolated Cu-phthalocyanine molecules chemisorbed on the Cu(111) surface based on conformational changes, previously identified via noise spectroscopy. By applying an appropriate bias voltage the molecules can either be prepared in their minimum energy configuration, or metastable ones, rotated by  $\pm 7^\circ$  and accompanied by opposite vertical displacements of orthogonal benzol rings. The underlying switching mechanism in dependence of the voltage sweep direction, as well as the extent to which the rotation direction can be controlled by the scan direction in repeated scans at reversed voltages, remains to be investigated.

## ACKNOWLEDGMENTS

The Swiss National Science Foundation (SNF), the European Union's Horizon 2020 research and innovation programme (ERC Advanced Grant No. 834402), the Swiss Nanoscience Institute, the Iran Science Elites Federation, the Joint Swiss-Polish Research Programme PSPB-085/2010, the COST Action MP1303, the Japan Society for the Promotion of Science (JSPS) KAKENHI Grant No. 15K21765, and the Japan Science and Technology Agency (JST) "Precursory Research for Embryonic Science and Technology (PRESTO)" for a project of "Molecular technology and creation of new function" are acknowledged for financial support. The computation time was provided by the Swiss National Supercomputing Center (CSCS).

- [1] A. Aviram and M. A. Ratner, *Chem. Phys. Lett.* **29**, 277 (1974).
- [2] C. Joachim, J. K. Gimzewski, and A. Aviram, *Nature (London)* **408**, 541 (2000).
- [3] A. Mänz, A. A. Hauke, and G. Witte, *J. Phys. Chem. C* **122**, 2165 (2018).
- [4] J. Lee, E. Lee, S. Kim, G. S. Bang, D. A. Shultz, R. D. Schmidt, M. D. E. Forbes, and H. Lee, *Angew. Chem. Int. Ed.* **50**, 4414 (2011).
- [5] J. C. Scott and L. D. Bozano, *Adv. Mater.* **19**, 1452 (2007).
- [6] I. Swart, T. Sonnleitner, and J. Repp, *Nano Lett.* **11**, 1580 (2011).
- [7] F. Mohn, L. Gross, N. Moll, and G. Meyer, *Nat. Nanotechnol.* **7**, 227 (2012).
- [8] N. Kocic, S. Decurtins, S.-X. Liu, and J. Repp, *J. Chem. Phys.* **146**, 092327 (2017).
- [9] R. Pawlak, A. Sadeghi, R. Jöhr, A. Hinaut, T. Meier, S. Kawai, Ł. Zajac, P. Olszowski, S. Godlewski, B. Such, T. Glatzel, S. Goedecker, M. Szymoński, and E. Meyer, *J. Phys. Chem. C* **121**, 3607 (2017).
- [10] L. L. Patera, F. Queck, P. Scheuerer, and J. Repp, *Nature (London)* **566**, 245 (2019).
- [11] L. L. Patera, F. Queck, P. Scheuerer, N. Moll, and J. Repp, *Phys. Rev. Lett.* **123**, 016001 (2019).
- [12] Z. J. Donhauser, B. A. Mantooth, K. F. Kelly, L. A. Bumm, J. D. Monnell, J. J. Stapleton, D. W. Price, A. M. Rawlett, D. L. Allara, J. M. Tour, and P. S. Weiss, *Science* **292**, 2303 (2001).
- [13] T. Kumagai, F. Hanke, S. Gawinkowski, J. Sharp, K. Kotsis, J. Waluk, M. Persson, and L. Grill, *Nat. Chem.* **6**, 41 (2013).
- [14] B. Borca, V. Schendel, R. Pétuya, I. Pentegov, T. Michnowicz, U. Kraft, H. Klauk, A. Arnau, P. Wahl, U. Schlickum *et al.*, *ACS Nano* **9**, 12506 (2015).
- [15] M. Ormaza, P. Abufager, B. Verlhac, N. Bachellier, M.-L. Bocquet, N. Lorente, and L. Limot, *Nat. Commun.* **8**, 1974 (2017).
- [16] J. Schütte, R. Bechstein, P. Rahe, H. Langhals, M. Rohlfing, and A. Kühnle, *Nanotechnology* **22**, 245701 (2011).
- [17] R. Pawlak, S. Fremy, S. Kawai, T. Glatzel, H. Fang, L.-A. Fendt, F. Diederich, and E. Meyer, *ACS Nano* **6**, 6318 (2012).

- [18] S. A. Burke, J. M. LeDue, J. M. Topple, S. Fostner, and P. Grütter, *Adv. Mater.* **21**, 2029 (2009).
- [19] S. J. van der Molen and P. Liljeroth, *J. Phys.: Condens. Matter* **22**, 133001 (2010).
- [20] R. Pawlak, T. Glatzel, V. Pichot, L. Schmidlin, S. Kawai, S. Fremy, D. Spitzer, and E. Meyer, *Nano Lett.* **13**, 5803 (2013).
- [21] P. Liljeroth, J. Repp, and G. Meyer, *Science* **317**, 1203 (2007).
- [22] F. Mohn, J. Repp, L. Gross, G. Meyer, M. S. Dyer, and M. Persson, *Phys. Rev. Lett.* **105**, 266102 (2010).
- [23] S. Fatayer, B. Schuler, W. Steurer, I. Scivetti, J. Repp, L. Gross, M. Persson, and G. Meyer, *Nat. Nanotechnol.* **13**, 376 (2018).
- [24] W. Auwärter, K. Seufert, F. Bischoff, D. Ecija, S. Vijayaraghavan, S. Joshi, F. Klappenberger, N. Samudrala, and J. V. Barth, *Nat. Nanotechnol.* **7**, 41 (2011).
- [25] V. D. Pham, J. Lagoute, O. Mouhoub, F. Joucken, V. Repain, C. Chacon, A. Bellec, Y. Girard, and S. Rousset, *ACS Nano* **8**, 9403 (2014).
- [26] G. Binnig, H. Rohrer, C. Gerber, and E. Weibel, *Phys. Rev. Lett.* **49**, 57 (1982).
- [27] G. Binnig, C. F. Quate, and C. Gerber, *Phys. Rev. Lett.* **56**, 930 (1986).
- [28] T. R. Albrecht, P. Grütter, D. Horne, and D. Rugar, *J. Appl. Phys.* **69**, 668 (1991).
- [29] O. Custance, R. Perez, and S. Morita, *Nat. Nanotechnol.* **4**, 803 (2009).
- [30] J. Bamidele, S. H. Lee, Y. Kinoshita, R. Turansky, Y. Naitoh, Y. J. Li, Y. Sugawara, I. Stich, and L. Kantorovich, *Nat. Commun.* **5**, 4476 (2014).
- [31] W. Steurer, J. Repp, L. Gross, I. Scivetti, M. Persson, and G. Meyer, *Phys. Rev. Lett.* **114**, 036801 (2015).
- [32] N. Pavliček and L. Gross, *Nat. Rev. Chem.* **1**, 0005 (2017).
- [33] R. Pawlak, S. Kawai, T. Meier, T. Glatzel, A. Baratoff, and E. Meyer, *J. Phys. D: Appl. Phys.* **50**, 113003 (2017).
- [34] J. I. Urgel, D. Ecija, W. Auwärter, and J. V. Barth, *Nano Lett.* **14**, 1369 (2014).
- [35] B. C. Stipe, *Science* **279**, 1907 (1998).
- [36] J. I. Pascual, N. Lorente, Z. Song, H. Conrad, and H.-P. Rust, *Nature (London)* **423**, 525 (2003).
- [37] S.-W. Hla, L. Bartels, G. Meyer, and K.-H. Rieder, *Phys. Rev. Lett.* **85**, 2777 (2000).
- [38] B. C. Stipe, M. A. Rezaei, W. Ho, S. Gao, M. Persson, and B. I. Lundqvist, *Phys. Rev. Lett.* **78**, 4410 (1997).
- [39] B. C. Stipe, M. A. Rezaei, and W. Ho, *Phys. Rev. Lett.* **81**, 1263 (1998).
- [40] S. Godlewski, H. Kawai, M. Kolmer, R. Zuzak, A. M. Echavarren, C. Joachim, M. Szymanski, and M. Saeys, *ACS Nano* **10**, 8499 (2016).
- [41] T. Sugimoto, Y. Kunisada, and K. Fukutani, *Phys. Rev. B* **96**, 241409(R) (2017).
- [42] V. D. Pham, V. Repain, C. Chacon, A. Bellec, Y. Girard, S. Rousset, E. Abad, Y. J. Dappe, A. Smogunov, and J. Lagoute, *ACS Nano* **11**, 10742 (2017).
- [43] T. Komeda, Y. Kim, M. Kawai, B. N. J. Persson, and H. Ueba, *Science* **295**, 2055 (2002).
- [44] M. Ohara, Y. Kim, and M. Kawai, *Phys. Rev. B* **78**, 201405(R) (2008).
- [45] S. Katano, Y. Kim, Y. Kagata, and M. Kawai, *J. Phys. Chem. C* **114**, 3003 (2010).
- [46] R. Pawlak, T. Meier, N. Renaud, M. Kisiel, A. Hinaut, T. Glatzel, D. Sordes, C. Durand, W.-H. Soe, A. Baratoff, C. Joachim, C. E. Housecroft, E. C. Constable, and E. Meyer, *ACS Nano* **11**, 9930 (2017).
- [47] H. Karacuban, M. Lange, J. Schaffert, O. Weingart, T. Wagner, and R. Möller, *Surf. Sci.* **603**, L39 (2009).
- [48] J. Schaffert, M. C. Cottin, A. Sonntag, H. Karacuban, C. A. Bobisch, N. Lorente, J.-P. Gauyacq, and R. Möller, *Nat. Mater.* **12**, 223 (2013).
- [49] J. Schaffert, M. C. Cottin, A. Sonntag, C. A. Bobisch, R. Möller, J.-P. Gauyacq, and N. Lorente, *Phys. Rev. B* **88**, 075410 (2013).
- [50] J. P. Perdew, K. Burke, and M. Ernzerhof, *Phys. Rev. Lett.* **77**, 3865 (1996).
- [51] S. Grimme, *J. Comput. Chem.* **27**, 1787 (2006).
- [52] P. E. Blöchl, *Phys. Rev. B* **50**, 17953 (1994).
- [53] G. Kresse and D. Joubert, *Phys. Rev. B* **59**, 1758 (1999).
- [54] G. Kresse and J. Hafner, *Phys. Rev. B* **47**, 558 (1993).
- [55] G. Kresse and J. Hafner, *Phys. Rev. B* **49**, 14251 (1994).
- [56] G. Kresse and J. Furthmüller, *Phys. Rev. B* **54**, 11169 (1996).
- [57] G. Kresse and J. Furthmüller, *Comput. Mater. Sci.* **6**, 15 (1996).
- [58] D. W. Pohl and R. Möller, *Rev. Sci. Instrum.* **59**, 840 (1988).
- [59] S. Kawai, T. Glatzel, S. Koch, A. Baratoff, and E. Meyer, *Phys. Rev. B* **83**, 035421 (2011).
- [60] S. Fremy, S. Kawai, R. Pawlak, T. Glatzel, A. Baratoff, and E. Meyer, *Nanotechnology* **23**, 055401 (2012).
- [61] S. W. Wu, N. Ogawa, and W. Ho, *Science* **312**, 1362 (2006).
- [62] J. Martínez-Blanco, C. Nacci, S. C. Erwin, K. Kanisawa, E. Locane, M. Thomas, F. von Oppen, P. W. Brouwer, and S. Fölsch, *Nat. Phys.* **11**, 640 (2015).
- [63] D. G. de Oteyza, A. El-Sayed, J. M. Garcia-Lastra, E. Goiri, T. N. Krauss, A. Turak, E. Barrena, H. Dosch, J. Zegenhagen, A. Rubio, Y. Wakayama, and J. E. Ortega, *J. Chem. Phys.* **133**, 214703 (2010).